

BAMBO: Construct Ability and Efficiency LLM Pareto Set via Bayesian Adaptive Multi-objective Block-wise Optimization

Kesheng Chen¹ Wenjian Luo¹ Zhenqian Zhu¹ Yamin Hu¹ Yiya Xi¹

Abstract

Constructing a Pareto set is pivotal for navigating the capability-efficiency trade-offs in Large Language Models (LLMs); however, existing merging techniques remain inadequate for this task. Coarse-grained, model-level methods yield only a sparse set of suboptimal solutions, while fine-grained, layer-wise approaches suffer from the “curse of dimensionality,” rendering the search space computationally intractable. To resolve this dichotomy, we propose **BAMBO** (Bayesian Adaptive Multi-objective Block-wise Optimization), a novel framework that automatically constructs the LLM Pareto set. BAMBO renders the search tractable by introducing a **Hybrid Optimal Block Partitioning** strategy. Formulated as a 1D clustering problem, this strategy leverages a dynamic programming approach to optimally balance intra-block homogeneity and inter-block information distribution, thereby dramatically reducing dimensionality without sacrificing critical granularity. The entire process is automated within an evolutionary loop driven by the q-Expected Hypervolume Improvement (qEHVI) acquisition function. Experiments demonstrate that BAMBO discovers a superior and more comprehensive Pareto frontier than baselines, enabling agile model selection tailored to diverse operational constraints. Code is available at: <https://github.com/xin8coder/BAMBO>.

1. Introduction

Large language models (LLMs) have revolutionized natural language processing by exhibiting remarkable reasoning abilities, often facilitated by chain-of-thought (CoT)

¹Guangdong Provincial Key Laboratory of Novel Security Intelligence Technologies, School of Computer Science and Technology, Harbin Institute of Technology, Shenzhen, China.. Correspondence to: Wenjian Luo <luowenjian@hit.edu.cn>.

prompting (Wei et al., 2022). However, extended reasoning sequences incur significant computational costs, including latency and resource consumption (Sui et al., 2025). To mitigate this, model merging has emerged as a promising technique to amalgamate specialized models—e.g., fusing a “Thinking” model with a base model into a unified entity that balances these competing objectives (Wu et al., 2025; Team et al., 2025).

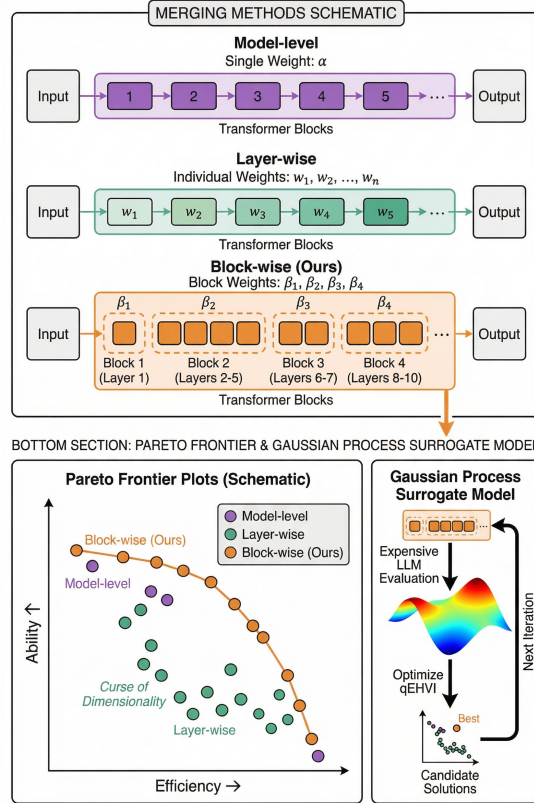


Figure 1. Schematic comparison of Pareto frontiers constructed via different merging granularities. BAMBO (Ours) achieves a denser and superior frontier compared to model-level and layer-wise approaches.

Constructing a Pareto set is essential for navigating the complex trade-offs between capability and efficiency in LLMs. Nevertheless, prevalent merging techniques predominantly focus on coarse-grained, model-level fusion. We observe

that these methods yield only a limited number of suboptimal solutions. Conversely, recent layer-wise optimization methods, utilizing evolutionary or Bayesian optimization, face a nearly intractable search space when applied to deep LLMs. To address these challenges, we propose **BAMBO**, an evolutionary multi-objective optimization framework designed to automatically construct the LLM Pareto set. Our framework circumvents the dimensionality issue by introducing a block-wise merging strategy, which significantly compresses the search space. To accurately assess model capabilities and ensure generalizability, we employ diverse benchmarks for specific performance evaluations. Furthermore, to guarantee stable and fair optimization across conflicting objectives, we formulate a normalized objective function based on established base and expert models. The process is automated within an evolutionary loop driven by the q-Expected Hypervolume Improvement (qEHVI) acquisition function, efficiently navigating the reduced space to identify the Pareto frontier. Experiments demonstrate that BAMBO discovers a superior and more comprehensive Pareto frontier than baselines, enabling rapid model selection for diverse operational constraints.

Existing merging strategies present a challenging trade-off between granularity and scalability. Traditional model-level methods, such as Task Arithmetic (Ilharco et al., 2022), TIES-Merging (Yadav et al., 2023), and DARE-Merging (Yu et al., 2024), apply a single interpolation weight per model. While computationally inexpensive, they are overly coarse and rely heavily on manual hyperparameter tuning, failing to systematically explore the trade-off landscape. Crucially, these methods cannot provide a continuous spectrum of trade-offs, generating only discrete solutions that restrict flexibility in practical deployment.

More recently, evolutionary computation-based methods (Akiba et al., 2025; Li et al., 2025) have adopted a more granular layer-wise approach. While offering finer control, this strategy faces a critical scalability barrier as LLM depth increases. The resulting explosion in search space dimensionality—the “curse of dimensionality”—renders optimization via surrogate models, such as Gaussian Processes, computationally infeasible.

To resolve this dilemma between coarse-grained simplicity and intractable fine-grained control, we propose BAMBO, a holistic framework enabling efficient, fine-grained model optimization. Our approach is built upon three interconnected innovations:

First, to create a manageable yet granular search space, we introduce **Hybrid Optimal Block Partitioning**. Unlike naive uniform partitioning, this strategy formulates layer grouping as a rigorous 1D clustering problem. By employing a **Dynamic Programming** algorithm that simultaneously optimizes for intra-block homogeneity (variance

minimization) and inter-block balance (information equalization), we achieve a “best-of-both-worlds” representation: more precise than model-level fusion, yet significantly more scalable than layer-wise optimization.

Second, to establish a mathematically sound basis for comparing conflicting goals, we define a **Normalized Objective Function**. This function standardizes the evaluation of diverse metrics, such as reasoning accuracy and token efficiency, by scaling them relative to pre-defined “expert” and “base” models, ensuring a stable and meaningful trade-off.

Finally, we develop an **Evolutionary Multi-objective Optimization Framework** to automate the search. Driven by Bayesian optimization with a Gaussian Process surrogate and the qEHVI acquisition function (Daulton et al., 2020), this framework efficiently navigates the reduced block-level search space to systematically construct the Pareto frontier.

Our contributions are as follows:

- A **Hybrid Optimal Block Partitioning** strategy that renders fine-grained model fusion tractable by reducing the high-dimensional search space of layer-wise parameters to a scalable, mathematically optimized block-level representation via Dynamic Programming.
- A normalized objective function that provides a principled method for evaluating and trading off conflicting capabilities on a standardized scale, enhancing optimization stability.
- An evolutionary multi-objective optimization framework that automates the discovery of optimal block-level interpolation weights, systematically constructing a Pareto set of models. We experimentally verify, for the first time, that model-level fusion methods are insufficient for constructing a high-quality LLM Pareto set.

2. Background

2.1. Model Merging Methods

Model merging is a technique that combines the parameters of multiple neural networks into a single model, often to amalgamate complementary capabilities (Yang et al., 2024) without requiring retraining from scratch. It differs from ensemble learning, which averages predictions during inference, by performing fusion directly at the parameter level, resulting in a unified model with reduced computational overhead. Common approaches include weight averaging, task arithmetic, and advanced methods like TIES-Merging. However, these methods are directly applied in model-level fusion algorithms, struggle with multi-task conflicts, and cannot construct a high-quality LLM Pareto set. Evolutionary algorithms have recently been applied to automate and

optimize the merging process.

Given a set of K models, $\{\mathcal{M}^{(1)}, \dots, \mathcal{M}^{(K)}\}$, that share a common architecture and are typically trained based on the same pre-trained model $\mathcal{M}^{(base)}$, the objective of model merging is to produce a new model, $\mathcal{M}^{(Merge)}$. Prominent approaches include:

Before evolutionary approaches, several representative parameter-level merging strategies were developed. Weight Averaging (Utans, 1996) interpolates model parameters to construct a unified model. Task Arithmetic (Ilharco et al., 2022) leverages task vectors to manipulate model behavior. TIES-Merging (Yadav et al., 2023) mitigates conflicts through sparsification and selective top-k parameter merging. DARE-Merging (Yu et al., 2024) reduces redundancy by randomly dropping and rescaling delta parameters. Breadcrumbs (Davari & Belilovsky, 2024) employs layer-wise masking to filter outliers and perturbations, while DELLA-Merging (Deep et al., 2024) adopts a Drop-Elect-Fuse framework to prune, select, and aggregate parameters more effectively. Although these methods enhance stability and efficiency, they still rely heavily on handcrafted hyperparameters and lack systematic mechanisms to explore trade-offs, fundamentally failing to address the shortcomings in searching for the LLM Pareto frontier.

To address these limitations, evolutionary computation-based methods have recently been introduced. TIES-DARE (Akiba et al., 2025) applies the Covariance Matrix Adaptation Evolution Strategy (CMA-ES) (Hansen et al., 2003) to automatically search for optimal merging configurations. It operates in two orthogonal spaces: parameter space merging, which optimizes layer-wise mixing coefficients and often integrates TIES-Merging with DARE for sparsification, focusing on single-objective optimization; and data flow space merging, which dynamically routes input tokens through layers of different models during inference, preserving original weights but requiring careful alignment to avoid distribution shifts. While effective for single-domain fusion, this method does not address multi-objective trade-offs.

In contrast, MO-MM (Li et al., 2025) formulates model merging as a multi-objective optimization problem. Leveraging Bayesian optimization with the qEHVI (Expected Hypervolume Improvement) (Daulton et al., 2020) acquisition function, MO-MM explores merging hyperparameters rather than layer-level weights, aiming for Pareto-optimal solutions across conflicting objectives such as code generation and mathematical reasoning. Moreover, it supports cross-domain fusion by jointly optimizing diverse tasks and incorporates an additional sparsity objective to mitigate overfitting. However, these methods primarily consider layer-wise optimization approaches. When dealing with large models that have a high number of layers, these methods face a series of difficulties, including an enormous search

space, expensive computational costs, and challenges in training surrogate models.

2.2. Multiobjective Optimization

Multiobjective optimization (MO) aims to find a set of solutions representing optimal trade-offs between conflicting objectives (Deb et al., 2002). The goal is to identify the Pareto frontier—solutions where no objective can be improved without degrading another. A multiobjective optimization problem (MOP) is formally defined as minimizing a vector of objective functions $F(X) = (f_1(X), f_2(X), \dots, f_m(X))$ subject to constraints, where X is a decision vector in the feasible region. Key concepts include:

- **Pareto Dominance:** A solution X dominates Y if $f_i(X) \leq f_i(Y)$ for all objectives and $f_j(X) < f_j(Y)$ for at least one objective.
- **Pareto Optimality:** A solution is Pareto optimal if no other solution dominates it.
- **Pareto Set (PS):** The set of all Pareto optimal solutions in the decision space.
- **Pareto Front (PF):** The image of the PS in the objective space, representing optimal trade-offs.

Bayesian optimization with acquisition functions like qEHVI (Daulton et al., 2020) has proven effective for expensive black-box functions, supporting parallel evaluations and constraint handling. qEHVI maximizes the expected hypervolume improvement, which measures the volume of space dominated by the PF relative to a reference point, enabling efficient exploration of the objective space.

3. Methodology

3.1. Problem Formulation

The goal of our work is to obtain the Pareto frontier of models under different efficiency constraints regarding reasoning ability and instruction-following capability as much as possible, so as to better trade-off different metrics. Therefore, obtaining the Pareto solution set composed of all possible fused models’ various capabilities is a logical premise, which we call the LLM Pareto set. The LLM Pareto set yields significant advantages. First, it allows for the rapid deployment of relevant models in various environments as needed without uneconomical retraining or model fine-tuning. On the other hand, this Pareto set can be combined with intelligent routing algorithms or directly according to user preference settings, thus enabling rapid switching to efficient models while minimizing performance loss.

Without loss of generality, here we discuss how to obtain a more ideal LLM Pareto set under given specific optimization

objectives. We formulate the model fusion problem as a multi-objective optimization problem with K objectives, as shown in below:

$$\min F(\mathcal{M}_{\text{merge}}) = (f_1(\mathcal{M}_{\text{merge}}), \dots, f_K(\mathcal{M}_{\text{merge}})). \quad (1)$$

Here, we treat the model fusion problem as a multi-objective optimization problem with K objectives. The optimization objective is to find a set of fused models $\{\mathcal{M}_{\text{merge}}\}$ that maximize the model capabilities $\{f_1, f_2, \dots, f_n\}$.

Before further giving the calculation method of the optimization objective function corresponding to the k -th model capability, for convenience of formal description, we define the evaluation benchmark set for the k -th model capability as $Q^{(k)}$, and the evaluation benchmark score set for model capabilities as $S^{(k)}$. Before fusion, we often use models that have been post-trained or fine-tuned in individual domains or for specific capabilities. Assume that the model fine-tuned specifically for the k -th capability is $\mathcal{M}_{\text{expert}}^{(k)}$, and the model without fine-tuning is $\mathcal{M}_{\text{base}}^{(k)}$.

In the field of LLMs, the estimation of model capabilities is often evaluated through different benchmarks. We can define the evaluation benchmark set for the k -th model capability as $Q^{(k)} = \{q_1^{(k)}, q_2^{(k)}, \dots, q_n^{(k)}\}$, where $q_n^{(k)}$ represents the n -th evaluation benchmark for the k -th model capability. Similarly, we can define the evaluation score mapping function for the benchmark set of the k -th model capability as $S^{(k)} = \{s_1^{(k)}(\mathcal{M}_{\text{merge}}), \dots, s_n^{(k)}(\mathcal{M}_{\text{merge}})\}$, where $s_n^{(k)}$ represents the evaluation score of the n -th benchmark for the k -th model capability. Based on the above definitions, we can give the calculation method for the optimization objective function corresponding to the k -th model capability as follows:

$$f_k(\mathcal{M}_{\text{merge}}) = \sum_{s^{(k)} \in S^{(k)}} \left(\frac{s^{(k)}(\mathcal{M}_{\text{merge}}) - s^{(k)}(\mathcal{M}_{\text{base}}^{(k)})}{s^{(k)}(\mathcal{M}_{\text{expert}}^{(k)}) - s^{(k)}(\mathcal{M}_{\text{base}}^{(k)})} \right). \quad (2)$$

Among them, $\mathcal{M}_{\text{merge}}$ can be obtained through different fusion methods, such as DARE, MI, etc. Here, we obtain it by dividing different layers for different Transformer blocks and using different weight parameters for model interpolation, as shown in the following equation:

$$\begin{aligned} \mathcal{M}_{\text{merge}} &= \text{Block-Wise-Merge}(\{\mathcal{M}_i\}; \beta_1^{(i)}, \dots, \beta_l^{(i)}); \\ \text{s.t. } \sum_i w_j^{(i)} &= 1, \quad \text{for } j = 1, \dots, l. \end{aligned} \quad (3)$$

Here, $\beta_1^{(i)}, \dots, \beta_k^{(i)}$ represent the aggregation weights for the k -th block of the i -th fused model.

3.2. Block-Wise Merge

In model fusion, existing interpolation or merging methods often treat domain-specific models as a whole. For example, parameter-space fusion is performed by assigning different global weights to each model, thereby obtaining merged models with different capabilities.

In recent evolutionary optimization-based model merging approaches, fusion parameters are assigned to each layer of the models, producing more diverse merged results and enabling the construction of a more comprehensive LLM Pareto set.

Evaluating the capabilities of merged models requires substantial computational resources. Therefore, surrogate models are necessary to approximate the mapping from decision variables to objective functions, assisting optimization algorithms. Gaussian process surrogates are particularly important, but traditional surrogate models face scalability issues when solving layer-wise multi-objective optimization problems for large models, since the number of decision variables grows rapidly (e.g., Qwen3-4B contains 36 Transformer layers).

Thus, reducing the number of decision variables is an intuitive strategy to lower the search difficulty in multi-model fusion. In this paper, we propose a block-wise merge method. This method assigns fusion parameters at the block level rather than the layer level, thereby reducing the dimensionality of the optimization problem and improving efficiency.

However, naive block partitioning (e.g., uniform averaging across layers) or simple greedy approaches face challenges. Prior work (Wu et al., 2025) and our experiments reveal that different Transformer layers contribute unequally to reasoning and efficiency. Furthermore, adjacent layers often exhibit similar parameter characteristics. An ideal partitioning strategy should satisfy two properties:

- **Homogeneity:** Layers within the same block should have similar difference magnitudes to share a common fusion weight.
- **Balance:** The total information ("difference mass") across blocks should be relatively balanced to ensure equal importance of decision variables.

To address this, we propose a **Hybrid Optimal Block Partitioning** strategy. We formulate the layer partitioning problem as a variation of the classic **Fisher-Jenks Natural Breaks optimization** (Jenks, 1967), which is essentially a **1D ordered clustering problem**. Unlike the standard Fisher-Jenks algorithm that solely minimizes within-class variance, our formulation incorporates a balance constraint to prevent the formation of trivial or overly large blocks.

Consider N models \mathcal{M} and a base model $\mathcal{M}_{\text{base}}$. For the i -th model and the l -th layer, we define the difference as:

$$\text{Diff}_l = \sum_{i=1}^N \left\| TV_l^{(i)} - TV_l^{\text{mean}} \right\|_p, \quad (4)$$

where $TV_l^{\text{mean}} = \frac{1}{N} \sum_{i=1}^N TV_l^{(i)}$.

Our objective is to find a partition $\mathcal{P} = \{B_1, \dots, B_K\}$ that minimizes a hybrid cost function J :

$$\min_{\mathcal{P}} J = \sum_{k=1}^K \text{Cost}(B_k) = \sum_{k=1}^K (\text{Var}(B_k) + \lambda \cdot \text{Dev}(B_k)), \quad (5)$$

where $\text{Var}(B_k)$ represents the within-block variance (homogeneity) and $\text{Dev}(B_k)$ represents the squared deviation from the target block sum (balance). Specifically:

$$\begin{aligned} \text{Var}(B_k) &= \sum_{l \in B_k} (\text{Diff}_l - \mu_{B_k})^2, \\ \text{Dev}(B_k) &= \left(\sum_{l \in B_k} \text{Diff}_l - \frac{1}{K} \sum_{j=1}^L \text{Diff}_j \right)^2. \end{aligned} \quad (6)$$

Here, μ_{B_k} is the mean difference of layers in block B_k , and λ is a hyperparameter. Since the cost function is *additive* over blocks, this problem possesses optimal substructure. We employ a Dynamic Programming (DP) algorithm to solve this optimization problem globally, ensuring the optimal partition is found in $O(K \cdot L^2)$ time. The detailed algorithm is shown in Algorithm 1, and the proof of optimality is provided in Appendix A.

3.3. Warm-Start Initialization

To enhance the efficiency and robustness of our Bayesian optimization, we employ a warm-start strategy during the initialization of the surrogate model. This strategy involves setting a higher initial evaluation budget (e.g., 8 evaluations compared to 4 evaluations per iteration) to ensure a more comprehensive initial exploration of the search space. The initial dataset is constructed by combining manually specified, high-potential configurations with additional samples generated via the Sobol sequence. Specifically, we introduce reference points corresponding to the "Thinking Model" and "Instruct Model," along with a balanced fusion of the two. The remaining initial evaluations are then populated with Sobol-initialized individuals, ensuring a diverse and well-distributed starting point for the optimization process.

3.4. Optimization Framework

We extend the MM-MO framework (Li et al., 2025) by embedding our block-wise partitioning and warm-start initialization into a Bayesian optimization loop. The core of our

Algorithm 1 Hybrid Optimal Block Partitioning

Input: Task vectors $TV_l^{(i)}$ for L layers, number of blocks K , balance weight λ
Output: Block partition $\mathcal{P} = \{B_1, \dots, B_K\}$
// 1. Compute Layer Differences
for $l = 1$ **to** L **do**
 $d_l \leftarrow \sum_{i=1}^N \|TV_l^{(i)} - \text{mean}(TV_l^{(i)})\|_p$
end for
 $Target \leftarrow (\sum d_l) / K$
// 2. Precompute Costs for all segments $[i, j]$
for $i = 1$ **to** L , $j = i$ **to** L **do**
 $Cost_{\text{var}}(i, j) \leftarrow \text{Variance}(d_{i\dots j}) \times (j - i + 1)$
 $Cost_{\text{bal}}(i, j) \leftarrow (\text{Sum}(d_{i\dots j}) - Target)^2$
 $Cost(i, j) \leftarrow Cost_{\text{var}}(i, j) + \lambda \cdot Cost_{\text{bal}}(i, j)$
end for
// 3. Dynamic Programming
Initialize $DP[k][l] \leftarrow \infty, DP[0][0] \leftarrow 0$
for $k = 1$ **to** K **do**
 for $l = 1$ **to** L **do**
 for $m = k - 1$ **to** $l - 1$ **do**
 if $DP[k - 1][m] + Cost(m + 1, l) < DP[k][l]$
 then
 $DP[k][l] \leftarrow DP[k - 1][m] + Cost(m + 1, l)$
 $Split[k][l] \leftarrow m$
 end if
 end for
 end for
end for
// 4. Backtrack to reconstruct blocks
Reconstruct \mathcal{P} from $Split$ matrix starting at $Split[K][L]$

framework is designed to efficiently navigate the block-wise search space and consists of two key repeating steps: fitting surrogate models and optimizing an acquisition function to select the next candidates.

Gaussian Process (GP) Surrogates. The relationship between the block-wise weights and the resulting (normalized) model performance is a black-box function that is expensive to evaluate. We employ separate Gaussian Process (GP) models for each objective as cheap-to-evaluate surrogates. The GP approximates this expensive mapping and, crucially, provides not only a mean prediction for any unevaluated configuration but also a principled uncertainty estimate, which is vital for balancing exploration and exploitation.

Acquisition Function Optimization. The search for new candidates is guided by the q-Expected Hypervolume Improvement (qEHVI) acquisition function (Daulton et al., 2020). The OptimizeAcquisition step involves numerically optimizing the qEHVI to find a batch of q candidate configurations that are collectively expected to yield the largest improvement to the current Pareto front's hypervolume (HV).

Algorithm 2 The BAMBO Optimization Framework

Input: Expert models $\{\mathcal{M}^{(i)}\}$, base model $\mathcal{M}_{\text{base}}$, number of blocks K , initial points N_0 , iterations T , acquisition batch size q

Output: Final Pareto set $\mathcal{X}_{\text{final}}$ and Pareto front $\mathcal{Y}_{\text{final}}$

// 1. Dimensionality Reduction via Block Partitioning

$\mathcal{B} \leftarrow \text{HybridOptimalBlockPartitioning}(\{\mathcal{M}^{(i)}\}, K)$

// 2. Warm-Start Initialization

Generate heuristic configurations $\mathcal{X}_{\text{setting}}$ (e.g., all-0, all-1 vectors)

Generate $\mathcal{X}_{\text{sobol}}$ with $(N_0 - |\mathcal{X}_{\text{setting}}|)$ Sobol points

$\mathcal{X}_0 \leftarrow \mathcal{X}_{\text{setting}} \cup \mathcal{X}_{\text{sobol}}$

$\mathcal{Y}_0 \leftarrow \text{EvaluateObjectives}(\mathcal{X}_0, \mathcal{B}, \{\mathcal{M}^{(i)}\}, \mathcal{M}_{\text{base}})$

// 3. Bayesian Optimization Loop

for $t = 0$ **to** $T - 1$ **do**

Fit Gaussian Process models $GP_t \leftarrow \text{FitGP}(\mathcal{X}_t, \mathcal{Y}_t)$

$\mathcal{X}_{\text{new}} \leftarrow \text{OptimizeAcquisition}(\text{qEHVI}, GP_t, q)$

$\mathcal{Y}_{\text{new}} \leftarrow \text{EvaluateObjectives}(\mathcal{X}_{\text{new}}, \mathcal{B}, \{\mathcal{M}^{(i)}\}, \mathcal{M}_{\text{base}})$

$\mathcal{X}_{t+1} \leftarrow \mathcal{X}_t \cup \mathcal{X}_{\text{new}}; \mathcal{Y}_{t+1} \leftarrow \mathcal{Y}_t \cup \mathcal{Y}_{\text{new}}$

end for

$(\mathcal{X}_P, \mathcal{Y}_P) \leftarrow \text{GetParetoFront}(\mathcal{X}_T, \mathcal{Y}_T)$

$(\mathcal{X}_{\text{final}}, \mathcal{Y}_{\text{final}}) \leftarrow \text{SelectSolution}(\mathcal{X}_P, \mathcal{Y}_P)$

This allows for both parallel evaluation and an intelligent search strategy that prioritizes promising regions of the search space.

Solution Selection. After obtaining the LLM Pareto set, an intuitive question is how to select an appropriate solution. A straightforward method is to calculate the cosine similarity between the normalized objective vectors \mathcal{Y}_P of the Pareto solutions and a user-defined preference vector, and then select the model with the best overall performance from the Top-K solutions with the highest cosine similarity. This ensures that the chosen model not only satisfies the performance distribution pattern under the user’s preference scenario but also maintains strong overall performance. In our experiments, we use the Das-Dennis method from the optimization field to generate a sufficient number of user preference vectors. Models are selected according to the above method based on these vectors. Additionally, we include the Pareto-optimal individuals that perform best from the perspective of each individual benchmark. The overall optimization process, which integrates these components, is summarized in Algorithm 2.

4. Experimental Setup

4.1. Models and Benchmarks

In this study, we formulate the optimization problem with two conflicting objectives: the reasoning capability objective function $f_{\text{reasoning}}$ and the model efficiency objective

function $f_{\text{efficient}}$. Our goal is to simultaneously maximize reasoning performance and computational efficiency by fusing a specialized ”Thinking” model, $\mathcal{M}_{\text{think}}$, with an efficiency-oriented ”Instruct” model, $\mathcal{M}_{\text{instruct}}$.

To evaluate these capabilities, we employ rigorous benchmarks including GPQA-Diamond (Rein et al., 2024) and AIME25. The specific model parameter settings and definitions are detailed in Table 1.

Reasoning Capability: We select the post-trained Thinking Model (e.g., Qwen3-4B-Thinking (Yang et al., 2025)) as the expert model for this dimension. Reasoning ability is assessed using the mathematical reasoning benchmark GPQA-Diamond and the scientific reasoning benchmark AIME25, with the average accuracy across these datasets serving as the performance metric.

Model Efficiency: We designate the post-trained Instruct Model (e.g., Qwen3-4B-Instruct (Yang et al., 2025)) as the expert model for efficiency, given its optimization for concise generation. Efficiency is quantified by the average output token count across the aforementioned reasoning benchmarks (GPQA-Diamond and AIME25), where a lower token count indicates higher efficiency.

To streamline the fusion process and enhance algorithmic efficiency, we employ only these two models for interpolation. Consequently, for the normalization of objectives, we simplify the definition of the ”base model” for each capability by using the opposing expert model (e.g., the based model serves as the base for reasoning, and the Thinking model serves as the base for efficiency).

Table 1. Multi-objective Model Interpolation Parameters Settings

OBJECTIVE	REASONING	EFFICIENCY
EXPERT MODEL	THINKING MODEL	INSTRUCT MODEL
BASE MODEL	INSTRUCT MODEL	THINKING MODEL
METRIC	MEAN ACCURACY (\uparrow)	MEAN TOKEN COUNT (\downarrow)
BENCHMARKS	{GPQA-DIAMOND, AIME25}	{GPQA-DIAMOND, AIME25}

4.2. Baselines

Task Arithmetic (Ilharco et al., 2022): Manipulates task vectors (the difference between fine-tuned and base models) to steer model behavior via arithmetic operations, enabling multi-task learning or knowledge forgetting. The task vector is defined as: $TV^{(i)} := \mathcal{M}^{(i)} - \mathcal{M}^{(\text{base})}$. Multiple capabilities can be combined by aggregating their task vectors and adding them back to the base model: $\mathcal{M}^{(\text{Merge})} = \mathcal{M}^{(\text{base})} + \alpha \sum_{i=1}^T TV^{(i)}$.

TIES-Merging (Yadav et al., 2023): Addresses parameter conflicts by sparsification, sign resolution, and selective merging. It retains only the top-k magnitude parameters in each layer to reduce interference. Multiple capabilities can

be combined as: $\mathcal{M}^{(\text{Merge})} = \mathcal{M}^{(0)} + \alpha \text{top-k}(TV^{(i)})$.

DARE-Merging (Yu et al., 2024): Introduces Drop And REscale (DARE) to sparsify delta parameters before merging. A proportion p of parameters is randomly dropped, and the remaining ones are rescaled by $1/(1-p)$. This reduces redundancy while preserving task-specific capabilities and mitigates interference across models. The merged model is defined as: $\mathcal{M}^{(\text{Merge})} = \mathcal{M}^{(\text{base})} + \alpha \sum_{i=1}^T \text{DARE}(TV^{(i)}, p)$.

Breadcrumbs (Davari & Belilovsky, 2024): Proposes a sparsification-and-masking strategy to construct multi-task models. For each task vector, layer-wise masks are applied to remove both large outliers and small perturbations, reducing noise and interference. Multiple capabilities can be combined as: $\mathcal{M}^{(\text{Merge})} = \mathcal{M}^{(\text{base})} + \alpha \sum_{i=1}^T m^{(i)} \cdot TV^{(i)}$, where $m^{(i)}$ is the mask filtering extreme tails of the weight distribution.

DELLA (Deep et al., 2024): Introduces Drop–Elect–Fuse via Magnitude (DELLA), a three-step framework for merging homologous models. It first applies MAGPRUNE, a magnitude-based pruning method that assigns higher dropout probabilities to smaller-magnitude parameters and rescales the surviving ones by $(1/(1-p))$. Then it elects delta parameters with consistent signs across experts to minimize directional conflicts, and finally fuses them by averaging and rescaling to form the merged model. The merged model is expressed as $\mathcal{M}^{(\text{Merge})} = \mathcal{M}^{(\text{base})} + \lambda \cdot \delta^{(\text{avg})}$, where $(\delta^{(\text{avg})})$ denotes the averaged and rescaled deltas after Drop–Elect–Fuse.

4.3. Experimental Settings

In our experiments, we compare our approach against all baseline methods (Task Arithmetic, TIES-Merging, DARE-Merging, Breadcrumbs, DELLA) applied at the model level. We use the same model settings as in our main experiments and obtain solution sets by interpolating with different weight combinations. From these sets, we identify Pareto-optimal individuals based on our defined objective functions. Given the large number of baseline algorithms and limited computational resources, we construct the solution sets for model-level algorithms using interpolation parameters ranging from 0.1 to 0.9 with an interval of 0.1. (In the Appendix, we provide a case study using Task Arithmetic with a finer interval setting—matching the total number of evaluations used by our block-wise method—but the results show no significant performance improvement for the Task Arithmetic algorithm).

Within our framework, any of the baseline methods can serve as the underlying fusion mechanism for our block-wise strategy; here, we select the simplest method, Task Arithmetic. regarding the block partitioning, we set the

number of blocks for all attention layers to 6. Additionally, the model’s embedding layer is treated as a separate block, and the final fully connected and normalization layers are grouped into another separate block, resulting in a total of 8 blocks. We set the number of initial individuals to 8 to prevent underfitting during the initialization of the surrogate model. The optimization process runs for 20 iterations, with a batch size of 4 samples evaluated per generation.

Furthermore, to validate the necessity of block-wise merging, we include a layer-wise comparison algorithm. Layer-wise merging can be viewed as an extreme case of block-wise merging where the number of blocks for attention layers equals the total number of attention layers. Apart from this difference, all other parameters remain identical, ensuring the layer-wise method uses the same total number of evaluations as the block-wise method.

For all model-level, block-wise, and layer-wise configurations, the inference parameters follow the official optimal settings for the Qwen3 model (Yang et al., 2025).

5. Results and Analysis

5.1. Block Partitioning

Figure 2 presents a comprehensive visualization of layer-wise differences and the proposed block partitioning strategies. The top two rows illustrate the L1-norm and L2-norm differences between the Qwen-4B base model and the Qwen-4B-Thinking model. We observe that the primary variations are concentrated in the deeper layers of the model. We hypothesize that this is because deeper layers are responsible for higher-level semantic processing, such as logical reasoning, whereas the differences in shallow layers handling elementary semantics are minimal. This finding aligns with and explains the observations in (Wu et al., 2025), where merging only the latter parts of the model was sufficient to switch the model into reasoning mode.

The bottom three rows compare different block partitioning strategies:

- The **Balance-only strategy** (3rd row) strictly enforces equal total difference per block, resulting in blocks with vastly different sizes (e.g., a single deep layer forming a block versus many shallow layers grouped together).
- The **Variance-only strategy** (4th row, standard Fisher-Jenks) focuses on grouping layers with similar difference magnitudes but may lead to imbalanced block importance.
- Our proposed **Hybrid strategy** (bottom row) achieves an optimal trade-off. It successfully isolates the highly

active deep layers into distinct blocks (preserving homogeneity) while maintaining a reasonable distribution of information mass across all blocks (ensuring balance).

This visualization confirms that our hybrid approach effectively captures the non-uniform distribution of task vector differences, providing a more rational initialization for the subsequent evolutionary optimization.

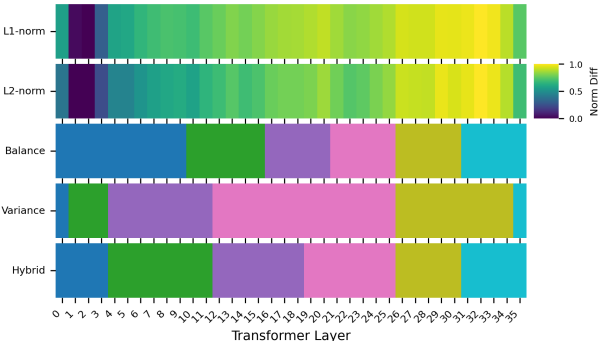


Figure 2. Layer-wise L1-norm and L2-norm differences between task models and the resulting block partition.

In our experiments, we selected 6 blocks. The bottom row depicts the partitioning results generated by our proposed algorithm. Layers with smaller differences in the earlier stages are grouped into larger blocks, while layers with significant differences in the later stages are divided into smaller blocks. This aligns with our design philosophy of dynamically allocating weights to reduce parameter redundancy while enhancing the granularity of critical decision variables.

5.2. Model-level Vs Layer-Wise Analysis

For each baseline algorithm, we conducted a grid search with varying parameter settings and evaluated all merged models to identify those forming the Pareto frontier. (We used a search space from 0.1 to 0.9 with a step size of 0.1; additional results with finer granularity matching our method’s evaluation budget are provided in the Appendix, yielding consistent conclusions). Figure 3 displays the distribution of these models in the objective function space, while Figures 5 and 4 illustrate their distribution in the metric spaces of AIME25 and GPQA-DIAMOND, respectively. Observing the results, it is evident that the Pareto solutions obtained via our framework dominate the collective Pareto frontier formed by all algorithms. Only a single solution from the Breadcrumbs algorithm appears on the frontier.

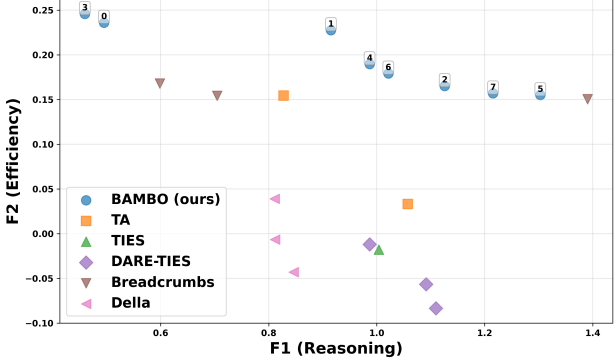


Figure 3. Distribution of merged models in the objective function space (f1 vs f2).

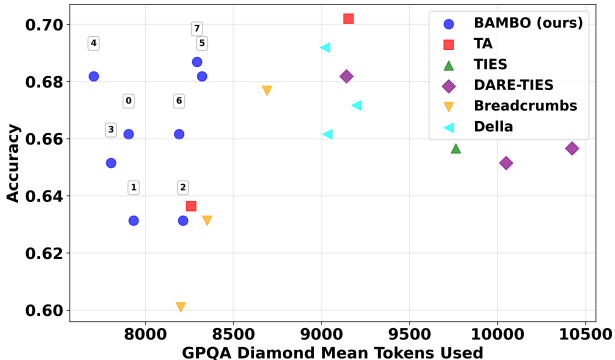


Figure 4. Pareto frontier analysis on GPQA-Diamond benchmark (Tokens vs Accuracy).

Critical Observation: Searching for model-level fusion weights via fine-grained grid search is insufficient to uncover the true Pareto frontier available from merging two models. Introducing fine-grained weight settings, such as layer-wise or block-wise strategies, is essential.

Table 2 presents the results of individuals obtained by different algorithms, detailing their corresponding objective functions and performance on respective datasets.

5.3. Solution Analysis

Figure 6 illustrates the Pareto frontier and non-Pareto individuals obtained by all algorithms. This demonstrates that our proposed method can rapidly identify the trade-offs of merged models within reasonable computational resource constraints. This provides an efficient implementation for rapid model customization based on user preferences. Based on this information, we can select efficient individuals using our proposed selection method. The sub-figure shows simulated user preference settings generated via uniform distribution. By comprehensively considering the align-

Table 2. Performance Comparison of Different Merging Methods

Method	ID	f1 (↑)	f2 (↑)	GPQA_ACC (↑)	GPQA_TOKENS (↓)	AIME25_ACC (↑)	AIME25_TOKENS (↓)	Pareto Solution
BAMBO (ours)	0	0.4949	0.2359	0.6616	7905	0.6333	15604	✓
	1	0.9152	0.2276	0.6313	7933	0.8000	15842	✓
	2	1.1259	0.1652	0.6313	8214	0.8667	17482	✓
	3	0.4595	0.2457	0.6515	7805	0.6333	15469	✓
	4	0.9868	0.1896	0.6818	7706	0.7666	17698	✓
	5	1.3030	0.1550	0.6818	8322	0.8667	17614	✓
	6	1.0215	0.1790	0.6616	8191	0.8000	17032	✓
	7	1.2154	0.1569	0.6869	8293	0.8333	17609	✓
TA	-	0.8276	0.1544	0.6364	8260	0.7666	17770	×
	-	1.0576	0.0330	0.7020	9154	0.7666	20201	×
TIES	-	1.0039	-0.0178	0.6566	9763	0.8000	20716	×
DARE-TIES	-	1.1094	-0.0835	0.6566	10423	0.8334	21653	×
	-	1.0915	-0.0567	0.6515	10048	0.8334	21498	×
	-	0.9868	-0.0120	0.6818	9142	0.7666	21845	×
Breadcrumbs	-	0.5983	0.1680	0.6010	8201	0.7333	17408	×
	-	0.7045	0.1542	0.6313	8351	0.7333	17579	×
	-	1.3906	0.1503	0.6768	8691	0.9000	16987	✓
Della	-	0.8108	0.0389	0.6717	19835	0.8000	28335	×
	-	0.8118	-0.0066	0.6616	9033	0.7333	20250	×
	-	0.8462	-0.0430	0.6919	9020	0.7000	21915	×

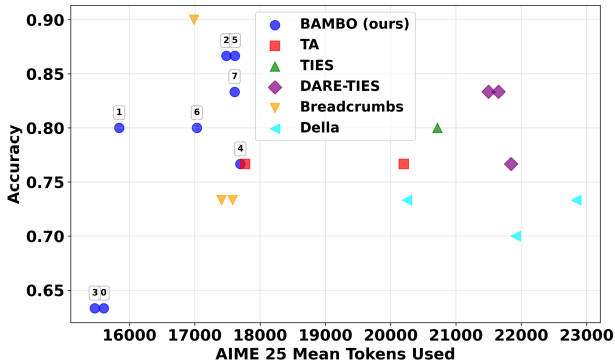


Figure 5. Pareto frontier analysis on AIME25 benchmark (Tokens vs Accuracy).

ment with user preferences and model capabilities, we can quickly adapt models for users given the obtained information. Furthermore, the acquisition of such a fine-grained Pareto frontier provides relevant information for dynamic adaptation strategies between model inference efficiency and capability, as well as for enhancing model capabilities under varying efficiency constraints.

5.4. Convergence Analysis

Figure 7 displays the performance of the best individuals in the solution set across different Pareto frontiers during iteration, the number of Pareto solutions obtained, and the changes in the HV indicator. These trends indicate that the block-wise partitioning strategy, combined with existing Bayesian optimization methods, is both effective and efficient.

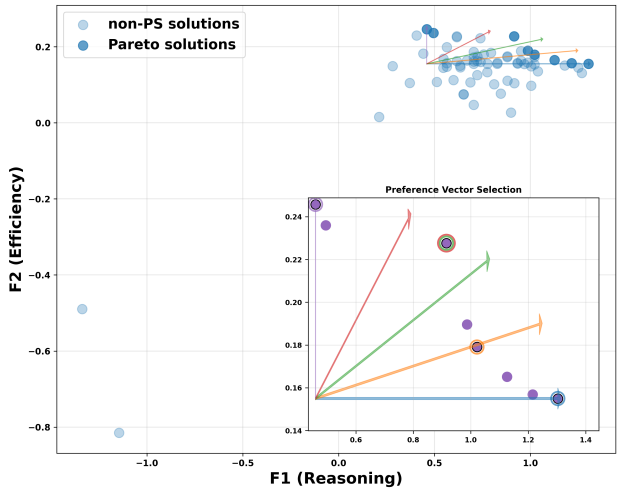


Figure 6. Visualization of Pareto frontier and non-Pareto individuals obtained by BAMBO.

6. Conclusion

In this paper, we addressed the critical challenge of balancing reasoning capability and computational efficiency in Large Language Models (LLMs). We identified that traditional model-level merging is insufficient for constructing a dense and high-quality Pareto frontier, while layer-wise optimization suffers from the "curse of dimensionality" and computational intractability. To overcome these limitations, we introduced BAMBO, a novel evolutionary multi-objective optimization framework.

Our contributions are threefold. First, we proposed a block-

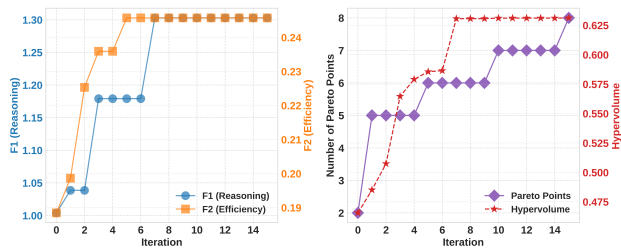


Figure 7. Convergence analysis: Hypervolume (HV) and Pareto set size over optimization iterations.

wise merging strategy that efficiently reduces the search space dimensionality by grouping layers based on task vector differences, making fine-grained optimization feasible. Second, we designed a normalized objective function anchored by expert and base models to ensure fair and stable trade-offs between conflicting objectives. Third, we integrated these components into an automated Bayesian optimization loop driven by the qEHVI acquisition function.

Extensive experiments on diverse benchmarks demonstrate that BAMBO significantly outperforms existing baselines, discovering a superior Pareto frontier with higher Hypervolume indicators. Our analysis confirms that block-wise merging effectively bridges the gap between coarse model-level fusion and expensive layer-wise optimization. Ultimately, BAMBO empowers users to dynamically select optimal models tailored to specific operational constraints, paving the way for more adaptive and efficient LLM deployment.

Impact Statement

This paper presents work whose goal is to advance the field of Machine Learning. There are many potential societal consequences of our work, none which we feel must be specifically highlighted here..

References

Akiba, T., Shing, M., Tang, Y., Sun, Q., and Ha, D. Evolutionary optimization of model merging recipes. *Nature Machine Intelligence*, 7(2):195–204, 2025.

Daulton, S., Balandat, M., and Bakshy, E. Differentiable expected hypervolume improvement for parallel multi-objective bayesian optimization. *Advances in neural information processing systems*, 33:9851–9864, 2020.

Davari, M. and Belilovsky, E. Model breadcrumbs: Scaling multi-task model merging with sparse masks. In *European Conference on Computer Vision*, pp. 270–287. Springer, 2024.

Deb, K., Pratap, A., Agarwal, S., and Meyarivan, T. A fast and elitist multiobjective genetic algorithm: Nsga-

ii. *IEEE transactions on evolutionary computation*, 6(2): 182–197, 2002.

Deep, P. T., Bhardwaj, R., and Poria, S. Della-merging: Reducing interference in model merging through magnitude-based sampling. *arXiv preprint arXiv:2406.11617*, 2024.

Hansen, N., Müller, S. D., and Koumoutsakos, P. Reducing the time complexity of the derandomized evolution strategy with covariance matrix adaptation (cma-es). *Evolutionary computation*, 11(1):1–18, 2003.

Ilharcó, G., Ribeiro, M. T., Wortsman, M., Gururangan, S., Schmidt, L., Hajishirzi, H., and Farhadi, A. Editing models with task arithmetic. *arXiv preprint arXiv:2212.04089*, 2022.

Jenks, G. F. The data model concept in statistical mapping. *International Yearbook of Cartography*, 7, 1967.

Li, B., Di, Z., Yang, Y., Qian, H., Yang, P., Hao, H., Tang, K., and Zhou, A. It’s morphing time: Unleashing the potential of multiple llms via multi-objective optimization. *IEEE Transactions on Evolutionary Computation*, 2025.

MacKay, D. J. et al. Introduction to gaussian processes. *NATO ASI series F computer and systems sciences*, 168: 133–166, 1998.

Rein, D., Hou, B. L., Stickland, A. C., Petty, J., Pang, R. Y., Dirani, J., Michael, J., and Bowman, S. R. Gpqa: A graduate-level google-proof q&a benchmark. In *First Conference on Language Modeling*, 2024.

Sui, Y., Chuang, Y.-N., Wang, G., Zhang, J., Zhang, T., Yuan, J., Liu, H., Wen, A., Zhong, S., Zou, N., et al. Stop overthinking: A survey on efficient reasoning for large language models. *arXiv preprint arXiv:2503.16419*, 2025.

Team, K., Du, A., Gao, B., Xing, B., Jiang, C., Chen, C., Li, C., Xiao, C., Du, C., Liao, C., et al. Kimi k1. 5: Scaling reinforcement learning with llms. *arXiv preprint arXiv:2501.12599*, 2025.

Utans, J. Weight averaging for neural networks and local resampling schemes. In *Proc. AAAI-96 Workshop on Integrating Multiple Learned Models*. AAAI Press, pp. 133–138. Citeseer, 1996.

Wei, J., Wang, X., Schuurmans, D., Bosma, M., Xia, F., Chi, E., Le, Q. V., Zhou, D., et al. Chain-of-thought prompting elicits reasoning in large language models. *Advances in neural information processing systems*, 35:24824–24837, 2022.

Wu, T., Yang, R., Liu, T., Wang, J., and Wong, N. Revisiting model interpolation for efficient reasoning. *arXiv preprint arXiv:2510.10977*, 2025.

Yadav, P., Tam, D., Choshen, L., Raffel, C. A., and Bansal, M. Ties-merging: Resolving interference when merging models. *Advances in Neural Information Processing Systems*, 36:7093–7115, 2023.

Yang, A., Li, A., Yang, B., Zhang, B., Hui, B., Zheng, B., Yu, B., Gao, C., Huang, C., Lv, C., et al. Qwen3 technical report. *arXiv preprint arXiv:2505.09388*, 2025.

Yang, E., Shen, L., Guo, G., Wang, X., Cao, X., Zhang, J., and Tao, D. Model merging in llms, mllms, and beyond: Methods, theories, applications and opportunities. *arXiv preprint arXiv:2408.07666*, 2024.

Yu, L., Yu, B., Yu, H., Huang, F., and Li, Y. Language models are super mario: Absorbing abilities from homologous models as a free lunch. In *Forty-first International Conference on Machine Learning*, 2024.

A. Proof of Optimality for Block Partitioning

In this section, we prove that the Dynamic Programming (DP) approach proposed in Section 3.3 guarantees finding the global minimum of the hybrid cost function J .

A.1. Problem Formulation

Let L be the total number of layers and K be the target number of blocks. Let d_1, d_2, \dots, d_L be the sequence of difference values for each layer. We aim to partition this sequence into K contiguous segments (blocks).

Let $\mathcal{C}(i, j)$ denote the cost of a single block containing layers from index i to j (inclusive, $1 \leq i \leq j \leq L$). Based on our definition:

$$\mathcal{C}(i, j) = \text{Var}(d_{i:j}) + \lambda \cdot \left(\sum_{t=i}^j d_t - \text{Target} \right)^2 \quad (7)$$

Since Target is a pre-calculated constant ($\frac{1}{K} \sum_{t=1}^L d_t$), the cost $\mathcal{C}(i, j)$ depends solely on the elements d_i, \dots, d_j .

The total cost for a partition into K blocks is the sum of the costs of individual blocks:

$$J = \sum_{k=1}^K \mathcal{C}(s_{k-1} + 1, s_k) \quad (8)$$

where $0 = s_0 < s_1 < \dots < s_K = L$ are the split points.

A.2. Optimal Substructure

Let $DP[k][l]$ be the minimum total cost to partition the first l layers into k blocks. The recurrence relation used in our algorithm is:

$$DP[k][l] = \min_{k-1 \leq m < l} \{DP[k-1][m] + \mathcal{C}(m+1, l)\} \quad (9)$$

Theorem: The value $DP[K][L]$ computed by this recurrence is the global minimum cost for partitioning L layers into K blocks.

Proof: We use induction and contradiction.

Base Case: For $k = 1$, $DP[1][l] = \mathcal{C}(1, l)$. Since there is only one way to partition the first l layers into 1 block, this is trivially optimal.

Inductive Step: Assume that for $k - 1$ blocks, the value $DP[k - 1][m]$ correctly represents the minimum cost for any $m < L$. We need to show that $DP[k][l]$ is optimal for k blocks.

Suppose, for the sake of contradiction, that there exists a partition of the first l layers into k blocks with a total cost J^* strictly less than $DP[k][l]$. Let the split points of this optimal partition be $0 = t_0 < t_1 < \dots < t_{k-1} < t_k = l$. The total cost can be decomposed as:

$$J^* = \text{Cost}(\text{First } k - 1 \text{ blocks}) + \mathcal{C}(t_{k-1} + 1, l) \quad (10)$$

where the "First $k - 1$ blocks" partition the layers 1 to t_{k-1} .

By our inductive hypothesis, $DP[k - 1][t_{k-1}]$ is the minimum possible cost to partition layers 1 to t_{k-1} into $k - 1$ blocks. Therefore:

$$\text{Cost}(\text{First } k - 1 \text{ blocks}) \geq DP[k - 1][t_{k-1}] \quad (11)$$

Substituting this back:

$$J^* \geq DP[k - 1][t_{k-1}] + \mathcal{C}(t_{k-1} + 1, l) \quad (12)$$

However, our DP recurrence explicitly calculates the minimum over all possible split points m , including t_{k-1} :

$$DP[k][l] = \min_m \{DP[k - 1][m] + \mathcal{C}(m + 1, l)\} \leq DP[k - 1][t_{k-1}] + \mathcal{C}(t_{k-1} + 1, l) \quad (13)$$

Thus, $DP[k][l] \leq J^*$. This contradicts the assumption that $J^* < DP[k][l]$. Therefore, $DP[k][l]$ must be the optimal cost. \square

A.3. Complexity Analysis

The computation of $\mathcal{C}(i, j)$ can be performed in $O(1)$ time using precomputed prefix sums and prefix square sums. The DP table has size $K \times L$. For each state, we iterate through $O(L)$ possible split points. Thus, the total time complexity is $O(K \cdot L^2)$. Given that L (number of layers, e.g., 32-80) and K (number of blocks, e.g., 4-8) are small constants in the context of LLMs, this algorithm is computationally negligible compared to model evaluation.

B. Details of Gaussian Process (GP) Surrogates

In the BAMBO framework, evaluating the objective functions (reasoning, efficiency, and instruction-following) for a given merging configuration is computationally expensive. To enable efficient optimization, we employ Gaussian Process (GP) (MacKay et al., 1998) surrogates to model the mapping from the block-wise merging weights to the normalized objective values.

B.1. Model Specification

Let $\mathbf{x} \in \mathbb{R}^D$ denote the decision variable vector, which corresponds to the block-wise merging weights $\{\beta_j^{(i)}\}$ defined in Equation (3). Due to our block-wise partitioning strategy, the dimensionality D is significantly reduced compared to layer-wise methods, making GP modeling computationally tractable and robust against overfitting.

We model each of the K objectives $f_k(\mathbf{x})$ ($k = 1, \dots, K$) independently using a Gaussian Process prior:

$$f_k(\mathbf{x}) \sim \mathcal{GP}(m_k(\mathbf{x}), k_k(\mathbf{x}, \mathbf{x}')), \quad (14)$$

where $m_k(\mathbf{x})$ is the mean function and $k_k(\mathbf{x}, \mathbf{x}')$ is the covariance kernel function. In our implementation, we use a constant mean function $m_k(\mathbf{x}) = \mu_k$.

B.2. Kernel Function

To capture the smoothness and non-linear correlations in the landscape of model merging, we utilize the Matern-5/2 kernel with Automatic Relevance Determination (ARD). The ARD kernel is particularly suitable for our block-wise approach as it learns separate length-scales for each block, effectively identifying which blocks contribute most significantly to specific capabilities (e.g., reasoning vs. efficiency). The kernel is defined as:

$$k_{\text{Matern}}(\mathbf{x}, \mathbf{x}') = \sigma_f^2 \left(1 + \sqrt{5}d + \frac{5}{3}d^2 \right) \exp(-\sqrt{5}d), \quad (15)$$

where $d = \sqrt{(\mathbf{x} - \mathbf{x}')^\top \Theta^{-2}(\mathbf{x} - \mathbf{x}')}$ is the weighted Euclidean distance, $\Theta = \text{diag}(\ell_1, \dots, \ell_D)$ is the diagonal matrix of length-scales for each block dimension, and σ_f^2 is the signal variance.

B.3. Model Fitting

Given the observed dataset $\mathcal{D}_t = \{(\mathbf{x}_i, \mathbf{y}_i)\}_{i=1}^{N_t}$ at iteration t , where \mathbf{y}_i represents the noisy observations of the objectives, we assume a Gaussian likelihood with homoscedastic noise σ_n^2 :

$$y_{i,k} = f_k(\mathbf{x}_i) + \epsilon_i, \quad \epsilon_i \sim \mathcal{N}(0, \sigma_n^2). \quad (16)$$

The hyperparameters $\{\mu_k, \sigma_f, \sigma_n, \Theta\}$ are estimated by maximizing the Log Marginal Likelihood (MLL):

$$\log p(\mathbf{y}|\mathbf{X}, \theta) = -\frac{1}{2}\mathbf{y}^\top (\mathbf{K} + \sigma_n^2 \mathbf{I})^{-1} \mathbf{y} - \frac{1}{2} \log |\mathbf{K} + \sigma_n^2 \mathbf{I}| - \frac{N}{2} \log 2\pi, \quad (17)$$

where \mathbf{K} is the covariance matrix computed on training data \mathbf{X} . We perform this optimization using L-BFGS-B to ensure the surrogate accurately reflects the current landscape before each acquisition step.

C. Details of Acquisition Function Optimization

To select the next batch of candidate configurations \mathcal{X}_{new} for parallel evaluation, we utilize the q -Expected Hypervolume Improvement (q EHVI) acquisition function, as proposed by Daulton et al. (2020). This method is chosen for its ability to handle noisy observations, constraints, and parallel candidate generation ($q > 1$) while being differentiable, allowing for efficient gradient-based optimization.

C.1. Hypervolume Indicator

The Hypervolume (HV) indicator measures the quality of a Pareto set \mathcal{P} by calculating the volume of the objective space dominated by \mathcal{P} and bounded by a reference point $\mathbf{r} \in \mathbb{R}^K$. Formally, let $A(\mathcal{P}, \mathbf{r}) = \bigcup_{\mathbf{y} \in \mathcal{P}} [\mathbf{r}, \mathbf{y}]$ be the union of hyper-rectangles dominated by \mathcal{P} . The hypervolume is defined as:

$$HV(\mathcal{P}, \mathbf{r}) = \lambda_K(A(\mathcal{P}, \mathbf{r})), \quad (18)$$

where λ_K denotes the Lebesgue measure in K -dimensional space. In our experiments, the reference point \mathbf{r} is dynamically set based on the worst observed values (nadir point) to ensure valid calculation.

C.2. q -Expected Hypervolume Improvement (q EHVI)

The classical EHVI computes the expected increase in hypervolume from a single new point. To leverage parallel computing resources, we seek a batch of q candidates $\mathbf{X}_{\text{cand}} = \{\mathbf{x}_1, \dots, \mathbf{x}_q\}$ simultaneously. The q EHVI is defined as the expectation of the hypervolume improvement over the joint posterior distribution of the candidates:

$$\alpha_{q\text{EHVI}}(\mathbf{X}_{\text{cand}}) = \mathbb{E}_{\mathbf{Y}_{\text{cand}} \sim \mathcal{P}(\cdot | \mathbf{X}_{\text{cand}}, \mathcal{D})} [HV(\mathcal{P} \cup \mathbf{Y}_{\text{cand}}) - HV(\mathcal{P})], \quad (19)$$

where \mathbf{Y}_{cand} are the posterior function values at \mathbf{X}_{cand} .

C.3. Gradient-Based Optimization via Reparameterization

A core contribution of Daulton et al. (2020) that we leverage is the ability to optimize \mathbf{X}_{cand} using exact gradients, rather than relying on gradient-free methods. This is achieved through the *reparameterization trick*.

The posterior joint distribution provided by our GP surrogate at \mathbf{X}_{cand} is multivariate normal: $\mathbf{Y}_{\text{cand}} \sim \mathcal{N}(\boldsymbol{\mu}(\mathbf{X}_{\text{cand}}), \boldsymbol{\Sigma}(\mathbf{X}_{\text{cand}}))$. Directly sampling \mathbf{Y}_{cand} would break the gradient flow. Instead, we express the samples as a deterministic transformation of a fixed, auxiliary noise source:

$$\mathbf{Y}_{\text{cand}}^{(s)} = \boldsymbol{\mu}(\mathbf{X}_{\text{cand}}) + \mathbf{L}(\mathbf{X}_{\text{cand}})\boldsymbol{\epsilon}^{(s)}, \quad \boldsymbol{\epsilon}^{(s)} \sim \mathcal{N}(0, \mathbf{I}), \quad (20)$$

where $\mathbf{L}(\mathbf{X}_{\text{cand}})$ is the Cholesky factor of the covariance matrix $\boldsymbol{\Sigma}(\mathbf{X}_{\text{cand}})$, and $\boldsymbol{\epsilon}^{(s)}$ are fixed samples drawn from a standard normal distribution using Sobol sequences to ensure low discrepancy.

By fixing $\boldsymbol{\epsilon}^{(s)}$, the acquisition function $\hat{\alpha}_{q\text{EHVI}}$ becomes a deterministic and differentiable function of the input decision variables \mathbf{X}_{cand} . The gradients can then be backpropagated through the entire computational graph:

- From the Hypervolume improvement to the sampled objectives $\mathbf{Y}_{\text{cand}}^{(s)}$ (via box decomposition derivatives);
- From $\mathbf{Y}_{\text{cand}}^{(s)}$ to the GP posterior parameters $\boldsymbol{\mu}$ and \mathbf{L} (via the linear reparameterization equation);
- From $\boldsymbol{\mu}$ and \mathbf{L} back to the inputs \mathbf{X}_{cand} (via the differentiable GP kernel and mean functions).

This allows us to maximize the acquisition function using standard gradient-based optimizers (e.g., L-BFGS-B or Adam) to efficiently find the optimal block-wise weights.